Polymer Chemistry

Accepted Manuscript

ROYAL SOCIETY OF CHEMISTRY

www.rsc.org/polymers

Cite this: DOI: 10.1039/c0xx00000x

www.rsc.org/xxxxxx

PAPER

Double Thermoresponsive Di- and Triblock Copolymers Based on *N*-vinylcaprolactam and *N*-vinylpyrrolidone: Synthesis and Comparative Study of Solution Behaviour

Anthony Kermagoret,[a] Kevin Mathieu,[a] Jean-Michel Thomassin,[a] Charles-André Fustin,[b] Roland Duchêne,[b] Christine Jérôme,[a] Christophe Detrembleur,[a] Antoine Debuigne[a,*]

Received (in XXX, XXX) Xth XXXXXXXXX 20XX, Accepted Xth XXXXXXXXX 20XX
DOI: 10.1039/b000000x

Poly(*N*-vinylcaprolactam) (P*N*VCL) and poly(*N*-vinylpyrrolidone) (P*N*VP) are water soluble polymers of interest especially in the biomedical field. Moreover, P*N*VCL is characterized by a lower critical solution temperature close to 36 °C in water, which makes it useful for the design of thermoresponsive systems. In this context, we used the cobalt-mediated radical polymerization (CMRP) and coupling reaction (CMRC) for synthesizing a series of well-defined *N*VCL and *N*VP-based copolymers, including statistical copolymers as well as double thermoresponsive diblocks and triblocks. Dynamic light scattering and turbidimetry analyses highlighted the crucial impact of the copolymer composition and architecture on the cloud point temperature (T_{CP}) of each segment but also their influence on the multistep assembly behaviour of block copolymers. Addition of NaCl enabled to adjust the inter-T_{CPS} temperature range of the di- and triblock in which selective precipitation of one block and self-assembly of the copolymer were favoured. Overall, data presented here provide a basis for the synthesis of a broad range of *N*VCL/*N*VP based copolymer architectures with tunable thermal response in water.

Introduction

Development of stimuli-responsive polymers, whose properties and solubility can be triggered by small changes in their environment (temperature, pH, electric or magnetic field, light, etc.), has become an important field of research in the last years.[1-3] These materials raised a great interest because they sustain a wide variety of applications notably in the biomedical area as bio-sensors, drug or gene delivery carriers or supports for tissue engineering, to name but a few.[4-6]

Temperature is very popular to regulate the solubility of the polymers[7-11] because no additive is required, the hydration/dehydration cycle can be repeated endlessly, at least under non degradative conditions for the polymer chain, and it is easily controllable. Some thermoresponsive polymers are only soluble in water upon heating above a given temperature called upper critical solution temperature (UCST) while others precipitate when heated above a given temperature called lower critical solution temperature (LCST).[12] Several common polymers exhibit a LCST behaviour in water including poly(oligoethylene glycol (meth)acrylate)s[13, 14], poly(propylene oxide),[15, 16] poly(vinylether)[17, 18] or poly(2-oxazoline)[19, 20] but the most studied sequence remains poly(N-isopropylacrylamide) (PNIPAM), which undergoes a coil-to-globule transition at 32 °C.[9, 21, 22] Nevertheless, poly(*N*-vinyl caprolactam) (P*N*VCL),[23-27] whose LCST (~36 °C) is close to the body temperature, has proved to be a valuable alternative to PNIPAM especially for biomedical applications.[23, 24] In contrast to PNIPAM, P*N*VCL does not produce toxic low-molecular-weight amines during hydrolysis and offers a higher biocompatibility as proved by cytotoxicity assays.[23, 24] Moreover, P*N*VCL does not exhibit a hysteresis phenomenon in the coil-to-globule-to-coil transition contrary to PNIPAM which forms interchain hydrogen bonds in the collapsed state.[21]

The solution behaviour dependence of P*N*VCL in function of the temperature has been thoroughly studied.[25-29] The LCST of this polymer is around 36 °C but it varies with the molar mass and the end-groups of the polymer.[25, 30-32] In this respect, controlled radical polymerization enables to tune the molar mass of the P*N*VCL but also to design statistical copolymers with precise *N*VCL content[33, 34] and copolymers containing one or more P*N*VCL segments.[34-43] Some CRP techniques have distinguished themselves for the controlled polymerization of *N*-vinyl amides and *N*VCL in particular,[44] i.e. the reversible addition fragmentation chain transfer (RAFT/MADIX),[30-33, 35-38] atom transfer radical polymerization[42, 43, 45, 46] and the organometallic-mediated radical polymerization (OMRP)[47, 48] based on cobalt complexes.[34, 39-41, 49] The latter is based on the reversible deactivation of the growing radical chains by the metal complex. In particular, bis-acetylacetonatocobalt(II) ($Co(acac)_2$) is a very efficient controlling agent for the polymerization of non-conjugated *N*-vinylamides including *N*VCL (Scheme 1).[49] Narrowly distributed P*N*VCL containing block copolymers with thermal induced self-assembly behaviour, like poly(vinyl acetate)-*b*-P*N*VCL and poly(vinyl alcohol)-*b*-P*N*VCL, were also prepared by OMRP.[39-41] The controlled statistical radical copolymerizations of *N*VCL with *N*-methyl vinyl acetamide (*N*MVA) or vinyl acetate (VAc) were also achieved by OMRP and the LCST of these copolymers could be precisely tuned up and down by incorporation of precise amounts of vinyl amide or vinyl ester comonomers, respectively.[34] After that, well-defined *N*VCL-based diblock having two LCSTs could also be prepared

by sequential OMRP of *N*VCL followed by the controlled copolymerization of *N*MVA with the residual amount of *N*VCL.[34] If examples of double thermoresponsive diblocks[9, 20, 34, 50] and of single thermoresponsive triblocks[15, 51-55] are rather common, only a handful of double thermoresponsive triblocks are reported[56-59] and none of them based on *N*VCL.

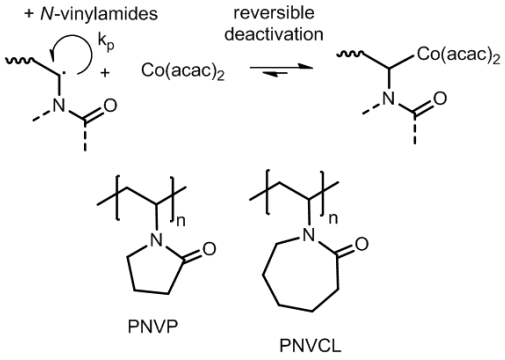

Scheme. 1 OMRP mechanism for *N*-vinylamides including *N*VCL and *N*VP.

Herein, we report the first synthesis of *N*VCL-based symmetrical ABA triblock copolymers having two discrete LCSTs. The latter are composed of P*N*VCL external blocks and a central block made of *N*VCL and *N*-vinyl pyrrolidone (*N*VP), i.e. P*N*VCL-*b*-P(*N*VCL-*co*-*N*VP)-*b*-P*N*VCL (Scheme 2). Briefly, the triblocks were obtained by isoprene-assisted bimolecular radical coupling[60-62] of the corresponding double thermo-responsive P*N*VCL-*b*-P(*N*VCL-*co*-*N*VP) diblocks formed by OMRP. A series of di- and triblocks with different block lengths were prepared in order to evaluate the relationship between the macromolecular features of the copolymer on the LCSTs and the self-assembly behaviour in water. A great advantage of the radical coupling approach is the fact that triblocks have the exact same block compositions compared to the parent diblocks from which they were generated but also the same length for the P*N*VCL blocks, which allows a direct comparative study of their thermal response.

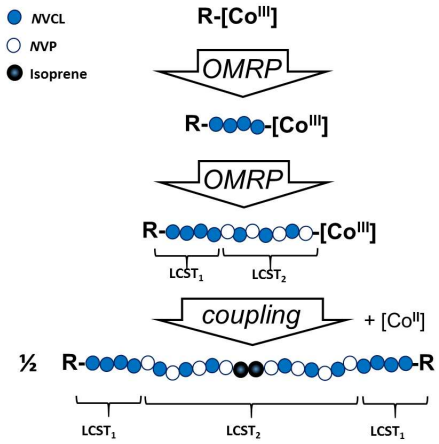

Scheme 2. General strategy for the synthesis of double thermo-responsive block copolymers by OMRP and radical coupling reaction.

Experimental Section

Materials

N-vinylpyrrolidone (*N*VP, >99 %, Aldrich) and isoprene (99 %, Aldrich) were dried over calcium hydride, degassed by two freeze-thawing cycles before distillation under reduced pressure and stored under argon. High purity *N*,*N*-dimethylformamide (DMF, >99%, Acros) and dichloromethane (CH_2Cl_2, 99,98%, Acros) are degassed by bubbling. *Bis*-(acetylacetonato)cobalt(II) (Co(acac)$_2$) (>98%, Acros) was stored under argon and used as received. 2,2,6,6-tetramethylpiperidine 1-oxyl (TEMPO, 98%, Aldrich) and *N*-vinylcaprolactam (*N*VCL, 98 %, Aldrich) were used as received. 2,2'-azobis(4-methoxy-2,4-dimethyl valeronitrile) (V-70, 96%, Wako) was stored at -20 °C and used as received. The alkyl-cobalt(III) adduct initiator ([Co(acac)$_2$-(CH(OAc)-CH$_2$)$_{\sim 4}$R$_0$]; R$_0$ being the primary radical generated by 2,2'-azo-bis(4-methoxy-2,4-dimethyl valeronitrile) (V-70, Wako) was prepared as described previously [63] and stored as a CH_2Cl_2 solution at -20 °C under argon.

Characterization

The molar masses (M_n) and molar mass dispersity (Đ) of the P(*N*VCL-*stat*-*N*VP) random copolymers were determined by size-exclusion chromatography (SEC) in dimethylformamide (DMF) containing LiBr (0.025 M) relative to polystyrene (PS) standards at 55 °C (flow rate: 1 mL/min) with a Waters 600 liquid chromatograph equipped with a 410 refractive index detector as well as two PSS GRAM analytical columns (1000 Å, 8*300 mm, particle size 10 µm) and one PSS GRAM analytical column (30 Å, 8*300 mm, particle size 10 µm). The absolute molar masses of the P*N*VCL-*block*-P(*N*VP-*stat*-*N*VCL) and P*N*VCL-*block*-P(*N*VP-*stat*-*N*VCL)-*block*-P*N*VCL block copolymers and their P*N*VCL precursors were determined by SEC equipped with a multiangle laser light scattering (MALLS) detector in DMF/LiBr (0.025 M). The Wyatt MALLs detector (120 mW solid-state laser, k ¼ 658 nm, DawnHeleos S/N342-H) measures the excess Rayleigh ratio R_h (related to the scattered intensity) at different angles for each slice of the chromatogram. The specific refractive index increment (d*n*/d*c*) of each (co)polymer was measured by using a Wyatt Optilab refractive index detector (k ¼ 658 nm). Data were processed with the Astra V software (Wyatt Technology). ^{1}H NMR spectra of reaction mixtures were recorded in $CDCl_3$ at 298 K with a 250 MHz Bruker spectrometer and ^{1}H NMR spectra of final polymers with a 400 MHz Bruker spectrometer.

Statistical cobalt-mediated radical copolymerization of *N*VCL and *N*VP. A bent 50 mL flask containing *N*VCL (9.18 g, 65.9 mmol) was connected to a 100 mL Schlenk equipped with a magnetic bar and degassed by three vacuum-argon cycles. The *N*VCL was melted at 40 °C under vacuum to eliminate oxygen. A solution of alkyl–cobalt(III) initiator ([Co(acac)$_2$-(CH(OAc)-CH$_2$)$_{\sim 4}$R$_0$] in CH_2Cl_2) was introduced under argon in the 100 mL Schlenk (1.0 mL of a 0.1 M stock solution, 0.1 mmol) and the dichloromethane was evaporated to dryness under reduced pressure at room temperature. The melted *N*VCL at 40 °C was then transferred onto the CMRP initiator before addition of distilled *N*VP (0.77 mL, 0.81 g, 7.3 mmol) under argon (*N*VP/*N*VCL molar feed ratio = 10/90, $M_{n\ th\ 100\%}$ = 100000

g/mol). The reaction mixture was stirred at 40 °C and the monomer conversion was monitored by ^{1}H NMR spectroscopy in $CDCl_3$. After 5.5 h, the monomer conversion reached 24% for *N*VCL and 17% for *N*VP. A volume of 1.5 mL of a degassed solution of TEMPO in DMF (1.5 mL of a 0.32 M stock solution, 0.48 mmol) was injected in the medium in order to stop the polymerization and eliminate the cobalt complex from the copolymer chain-end, according to a previous report.[64] The mixture was dissolved in approximately 20 mL of DMF and the polymer was recovered by precipitation in diethylether (Et_2O, 200 mL). The polymer was then filtered, dried under reduced pressure and purified by dialysis overnight in deionized water using a Spectra/Por®1 membrane (6-8 kD, 8 mL/cm). The final P(*N*VCL-*stat*-*N*VP) copolymer was collected as a white powder after lyophilization of the aqueous solution. The molecular parameters of the copolymer were measured by SEC in DMF using PS as a calibration ($M_{n\ SEC}$ = 28900 g/mol, Đ = 1.05). The composition of the copolymer previously dissolved in D_2O and dry at 60 °C overnight was determined by ^{1}H NMR (400 MHz) in $CDCl_3$ (*N*VCL/*N*VP molar ratio in the copolymer = 82/18) (see Figure S1)

Similar experiments were carried out with various *N*VCL/*N*VP molar ratios (see Table 1). The molecular parameters of the copolymers were measured by SEC in DMF using PS as a calibration: *N*VCL/*N*VP molar ratio in the copolymer = 73/27, $M_{n\ SEC}$ = 24900 g/mol, Đ = 1.06 ; *N*VCL/*N*VP molar ratio in the copolymer = 58/42, $M_{n\ SEC}$ = 22000 g/mol, Đ = 1.10 ; *N*VCL/*N*VP molar ratio in the copolymer = 51/49, $M_{n\ SEC}$ = 33600 g/mol, Đ = 1.10 ; *N*VCL/*N*VP molar ratio in the copolymer = 43/57, $M_{n\ SEC}$ = 40400 g/mol, Đ = 1.12 ; *N*VCL/*N*VP molar ratio in the copolymer = 28/72, $M_{n\ SEC}$ = 29300 g/mol, Đ = 1.24 ; Data are presented in Table 1.

Synthesis of the P*N*VCL-*block*-P(*N*VCL-*stat*-*N*VP) diblock copolymer $C_{132}(C_{40}P_{172})$. A bent 50 mL flask containing *N*VCL (15.0 g, 107.7 mmol) was connected to a 100 mL Schlenk equipped with a magnetic bar and degassed by three vacuum-argon cycles. The *N*VCL was melted at 40 °C under vacuum to eliminate oxygen. A solution of alkyl–cobalt(III) initiator ($[Co(acac)_2\text{-}(CH(OAc)\text{-}CH_2)_{\sim 4}R_0]$ in CH_2Cl_2) was introduced under argon in the 100 mL Schlenk (3 mL of a 0.1 M stock solution, 0.3 mmol) and the dichloromethane was evaporated to dryness under reduced pressure at room temperature. The melted *N*VCL at 40 °C was then transferred onto the CMRP initiator ($M_{n\ th\ 100\%}$ = 100000 g/mol). The reaction mixture was heated at 40 °C under stirring and ^{1}H NMR analyses of aliquots were carried out to follow the monomer conversion. When the *N*VCL consumption reached 27%, a sample was picked out of the medium, diluted in DMF containing LiBr and added with traces of TEMPO before SEC-MALLS analysis (d*n*/d*c* of P*N*VCL = 0.0916 mL/g, $M_{n\ MALLS}$ = 18400 g/mol, $Đ_{MALLS}$ = 1.03 and Đ = 1.05 with the PS calibration). Then, *N*VP (13.7 mL, 14.28 g, 128.0 mmol) was added under argon to the reaction mixture with the residual *N*VCL and the polymerization was pursued at 40 °C (comonomer feed *N*VP/*N*VCL: 63/37). After 2 h, the mixture became viscous. Based on the ^{1}H NMR spectrum of the reaction mixture in $CDCl_3$, the *N*VP consumption reached 19% and the cumulative *N*VCL conversion was 43%. A volume of 25 mL of DMF was added to decrease the viscosity. Half of the solution was further used for the synthesis of the triblock (see procedure below) while the rest was transferred using a cannula to another 100 mL Schlenk containing 100 mg of TEMPO (0.64 mmol, degassed by three vacuum-argon cycles) in order to produce the cobalt-free P*N*VCL-*block*-P(*N*VCL-*stat*-*N*VP) diblock. After treatment with TEMPO, the diblock was precipitated in diethylether (250 mL), filtered, dried and purified by dialysis using a Spectra/Por®1 membrane (6-8 kD) in deionized water. The P*N*VCL-*block*-P(*N*VCL-*stat*-*N*VP) copolymer was collected as a white powder after lyophilization of the aqueous solution. SEC-MALLS measurements were carried out in DMF in order to determine the molecular parameters of the copolymer (d*n*/d*c* of P*N*VCL-*block*-P(*N*VCL-*stat*-*N*VP) = 0.0992 mL/g, $M_{n\ MALLS}$ = 43100 g/mol, $Đ_{MALLS}$ = 1.05 and Đ = 1.08 with PS calibration). The composition of P(*N*VCL-*stat*-*N*VP) block was determined by ^{1}H NMR (81/19 : *N*VCL/*N*VP) and allowed to attribute the degree of polymerization of each segment of the copolymer ($PNVCL_{132}$-*block*-$P(NVCL_{40}$-*stat*-$NVP_{172})$).

Synthesis of P*N*VCL-*block*-P(*N*VCL-*stat*-*N*VP)-*block*-P*N*VCL block copolymers $C_{132}(C_{80}P_{344})C_{132}$. The above mentioned P*N*VCL-*block*-P(*N*VCL-*stat*-*N*VP)-$Co(acac)_2$ diblock (0.15 mmol) in DMF (12.5 mL) was reacted with 2 mL of isoprene (1.36 g, 20.0 mmol) at room temperature overnight in order to produce the triblock counterpart by radical coupling reaction.[60-62] The resulting P*N*VCL-*block*-P(*N*VCL-*stat*-*N*VP)-*block*-P*N*VCL triblock copolymer was precipitated in diethylether (250 mL), filtered, dried and purified by dialysis using a Spectra/Por®1 membrane (6-8 kD) in deionized water. It was then collected as a white powder after lyophilization of the aqueous solution. SEC-MALLS measurements in DMF containing LiBr (0.025 M) determine the molecular parameters of the copolymer (d*n*/d*c* of P*N*VCL-*block*-P(*N*VCL-*stat*-*N*VP)-*block*-P*N*VCL = 0.0969 mL/g $M_{n\ MALLS}$ = 71900 g/mol, $Đ_{MALLS}$ = 1.19 and Đ = 1.24 (calibration PS)). The composition of P(*N*VCL-*stat*-*N*VP) block is the same than the diblock (entry 2 in Tables 2 and S1).

A series of P*N*VCL-*block*-P(*N*VCL-*stat*-*N*VP) diblock and P*N*VCL-*block*-P(*N*VCL-*stat*-*N*VP)-*block*-P*N*VCL copolymers with different block length and composition have been prepared accordingly (see Tables 2 and S1 for molecular characteristics and polymerization conditions). In order to distinguish the P*N*VCL-*block*-P(*N*VCL-*stat*-*N*VP) and P*N*VCL-*block*-P(*N*VCL-*stat*-*N*VP)-*block*-P*N*VCL copolymers based on their composition, $\mathbf{C_n(C_lP_m)}$ and $\mathbf{C_n(C_{2l}P_{2m})C_n}$ labels were used where **C** and **P** correspond to *N*V**C**L and *N*V**P**, respectively, and $_\mathbf{n}$ and $_\mathbf{l}$ denoted the number of *N*VCL units and $_\mathbf{m}$ the number of *N*VP units.

$C_{68}(C_{74}P_{191})$ & $C_{68}(C_{148}P_{382})C_{68}$ (entry 1 in Tables 2 and S1) **:** $M_{n\ MALLS}$ P*N*VCL = 9500 g/mol, $Đ_{MALLS}$ = 1.04, d*n*/d*c* = 0.0916 mL/g, Đ = 1.07 (calibration PS), $M_{n\ MALLS}$ P*N*VCL-*block*-P(*N*VCL-*stat*-*N*VP) = 41400 g/mol, $Đ_{MALLS}$ = 1.05, Đ = 1.13 (calibration PS), d*n*/d*c* = 0.0872 mL/g, *N*VCL/*N*VP molar ratio in the statistical copolymer = 72/28, d*n*/d*c* = 0.0951 mL/g, $M_{n\ MALLS}$ P*N*VCL-*block*-P(*N*VCL-*stat*-*N*VP)-*block*-P*N*VCL = 64500 g/mol, $Đ_{MALLS}$ = 1.16, Đ = 1.24 (calibration PS).

$C_{236}(C_{55}P_{154})$ & $C_{236}(C_{110}P_{308})C_{236}$ (entry 3 in Tables 2 and S1):

$M_{n\ MALLS}$ P*N*VCL = 32800 g/mol, $Đ_{MALLS}$ = 1.04, Đ = 1.06 (calibration PS), d*n*/d*c* = 0.0916 mL/g, $M_{n\ MALLS}$ P*N*VCL-*block*-P(*N*VCL-*stat*-*N*VP) = 57500 g/mol, $Đ_{MALLS}$ = 1.05, Đ = 1.06 (calibration PS), d*n*/d*c* = 0.0906 mL/g, *N*VCL/*N*VP molar ratio in the statistical copolymer = 74/26, d*n*/d*c* = 0.0906 mL/g, $M_{n\ MALLS}$ P*N*VCL-*block*-P(*N*VCL-*stat*-*N*VP)-*block*-P*N*VCL = 110500 g/mol, $Đ_{MALLS}$ = 1.06, Đ = 1.13 (calibration PS).

$C_{282}(C_{27}P_{297})$ & $C_{282}(C_{54}P_{594})C_{282}$ (entry 4 inTables 2 and S1)**:** $M_{n\ MALLS}$ P*N*VCL = 39200 g/mol, $Đ_{MALLS}$ = 1.05, Đ = 1.06 (calibration PS), d*n*/d*c* = 0.0916 mL/g, $M_{n\ MALLS}$ P*N*VCL-*block*-P(*N*VCL-*stat*-*N*VP) = 76200 g/mol, $Đ_{MALLS}$ = 1.09, Đ = 1.08 (calibration PS), dn/dc = 0.0867 mL/g, *N*VCL/*N*VP molar ratio in the statistical copolymer = 8/92, dn/dc = 0.0849 mL/g, $M_{n\ MALLS}$ P*N*VCL-*block*-P(*N*VCL-*stat*-*N*VP)-*block*-P*N*VCL = 127700 g/mol, $Đ_{MALLS}$ = 1.14, Đ = 1.13 (calibration PS).

Aqueous solution behaviour. The transmittance of the aqueous solutions of polymers (1 g/L and 10 g/L) was recorded on a Jasco V630 UV-vis spectrophotometer at 700 nm equipped with a temperature controller system (ETCS-761). The heating/cooling rate was 1 °C/min between 25 °C and 85 °C. The cloud point temperature (T_{CP}) was defined at the half drop transmittance from the initial transmittance. DLS experiments were performed on a Malvern CGS-3 apparatus equipped with a He-Ne laser with a wavelength of 633 nm. The measurements were performed in water at 90 ° angle at a concentration of 1 g/L. Data were analysed using the CONTIN method, which is based on an inverse-Laplace transformation of the data and gives access to a size distribution histogram.

Results and Discussion

Copolymer synthesis by CMRP

The first part of the discussion section is exclusively dedicated to the synthesis of the *N*VCL and *N*VP containing statistical, diblock and symmetrical triblock copolymers. The control of the radical copolymerization of this pair of *N*-vinylamides using $Co(acac)_2$ as mediating species will be presented as well as the macromolecular features of each copolymer like composition, block length, dispersity, etc. The solution behaviour and the thermal response of these copolymers will be addressed and compared in the next section. Nevertheless, when reading through the synthesis section, it is interesting to keep in mind that increasing the *N*VP content in a P*N*VCL backbone is expected to increase the LCST of the polymer segment because P*N*VP is more hydrophilic than P*N*VCL and does not exhibit LCST in pure water.[65]

First, the controlled statistical radical copolymerization of *N*VCL and *N*VP was performed in bulk at 40 °C by CMRP using a low molecular weight alkyl-cobalt(III) adduct (R-$Co(acac)_2$) as initiator. The latter consists of oligoPVAc (average number of 4 VAc units) capped by $Co(acac)_2$ whose synthesis and ability to initiate the CMRP of *N*-vinylamides has been previously reported.[49] Upon heating, homolytic cleavage of the R-$Co(acac)_2$ bond occurs releasing the initiating fragment (R•) and the metallic controlling agent which reversibly traps the growing radical chains. Table 1 summarizes the *N*VP/*N*VCL statistical copolymers prepared in this study. Several comonomer feed ratios were tested and the monomer/initiator molar ratio was adjusted to target P(*N*VCL-*stat*-*N*VP) copolymer of 100000 g/mol at full monomer conversion. Although CMRP of *N*VCL remains efficient above 60%,[49] the above mentioned *N*VP/*N*VCL copolymerizations were stopped between 20% and 35% in order to ensure an optimal control of the polymerization and well-defined *N*VP/*N*VCL statistical copolymers with molar masses ranging between 20000 and 40000 g/mol were produced accordingly. In this case, the dispersity of the copolymers slightly increases with the *N*VP content in the feed. This observation is consistent with the better control reported for the *N*VCL homopolymerization compared to the *N*VP under the same experimental conditions.[49] The compositions of the resulting copolymers were determined by ^{1}H NMR (see Figure S1). The *N*VP content was systematically a bit higher in the copolymer than in the feed, which is in good agreement with reactivity ratio reported in the literature (r_{NVCL} = 1.7, r_{NVP} = 2.8).[66]

Table 1. Statistical cobalt-mediated radical copolymerization of *N*VCL and *N*VP in bulk at 40 °C.

Entry	In the feed (mol %) *N*VP/*N*VCL	[monomers]/[R-$Co(acac)_2$]	Time (h)	Conv. (%) [a]		M_n (g/mol)[b]	Đ [b]	In the copolymer (mol %) [c] *N*VP/*N*VCL
				*N*VCL	*N*VP			
1	10/90	731	5.5	24	17	28900	1.05	18/82
2	20/80	747	5	22	22	24900	1.06	27/73
3	30/70	759	4	22	34	22000	1.10	42/58
4	40/60	780	5.5	30	24	33600	1.10	49/51
5	50/50	803	5	25	35	40400	1.12	57/43
6	60/40	803	5.5	34	29	29300	1.24	72/28

[a] Determined by ^{1}H NMR 250 MHz in $CDCl_3$. [b] Determined by SEC in DMF containing LiBr (Calibration PS). [c] Determined by ^{1}H NMR 400 MHz in $CDCl_3$.

Next, CMRP and CMRC methods were used to produce novel double thermoresponsive *N*VCL and *N*VP-based diblocks and triblocks (Scheme 3). Inspired by a recent one-pot procedure for the copolymerization of *N*VCL and *N*MVA,[34] our general strategy consists in the controlled radical homopolymerization of *N*VCL from R-Co(acac)$_2$ in bulk at 40 °C up to 27% of conversion followed by injection of a precise amount of *N*VP which copolymerizes with the residual *N*VCL leading to the targeted P*N*VCL-*block*-P(*N*VCL-*stat*-*N*VP)-Co(acac)$_2$. After dilution with dimethylformamide, the resulting P*N*VCL-*block*-P(*N*VCL-*stat*-*N*VP)-Co(acac)$_2$ copolymer solution was divided in two equal parts. One of them was treated with TEMPO in order to eliminate the metal at the chain-end of the P*N*VCL-*block*-P(*N*VCL-*stat*-*N*VP) diblock. The other portion was reacted at room temperature with an excess of isoprene compared to the cobalt promoting the radical coupling of the diblock by CMRC and the formation of the corresponding P*N*VCL-*block*-P(*N*VCL-*stat*-*N*VP)-*block*-P*N*VCL triblock. Briefly, the allyl radical resulting from the addition of one isoprene unit at the copolymer chain-end is not prone to propagate at room temperature nor to react with the Co(acac)$_2$. Consequently, massive dimerization of these allyl radicals terminated chains occurs.[60-62, 67] Importantly, the degree of polymerization of the P*N*VCL block and composition of the P(*N*VCL-*stat*-*N*VP) segment are identical in the triblocks and the parent diblocks, which is a serious advantage for comparing the thermal properties of both architecture, as will be discussed later.

Table 2 summarizes the molecular parameters (M_n, DP, Đ) of the P*N*VCL precursors, the P*N*VCL-*block*-P(*N*VCL-*stat*-*N*VP) diblocks and the final P*N*VCL-*block*-P(*N*VCL-*stat*-*N*VP)-*block*-P*N*VCL triblocks. Detailed polymerization conditions are provided in the experimental section and in Table S1. The exact molar mass of the polymers was obtained by DMF-SEC chromatography equipped with a multi-angle laser light scattering (MALLS) detector and the Đ using a PS calibration. The composition of the P(*N*VCL-*stat*-*N*VP) statistical segment in the diblock and the triblock was determined by ^{1}H NMR by taking into account the degree of polymerization of the P*N*VCL block that it is linked to.

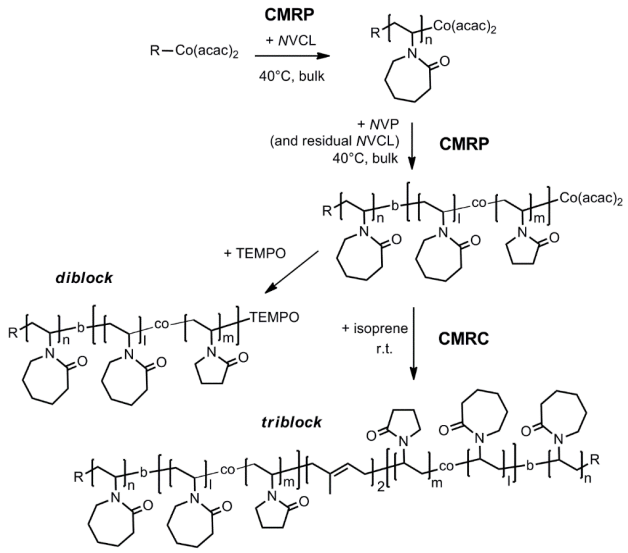

Scheme 3. Synthesis of *N*VCL and *N*VP containing diblock and triblock by CMRP and CMRC.

The low dispersity of the polymers, the composition of the statistical segment and the increase of molar mass at each step of the process provide a reliable basis to conclude on the efficacy of this synthetic approach. The overlay of the chromatograms in Figure 1 confirms the efficiency of the P*N*VCL-*block*-P(*N*VCL-*stat*-*N*VP) by chain extension carried out from the P*N*VCL-Co(acac)$_2$. Although not quantitative, the radical coupling reaction is efficient because the molar mass of a large majority of the chains double when treating the P*N*VCL-*block*-P(*N*VCL-*stat*-*N*VP)-Co(acac)$_2$ with isoprene. Indeed, a limited amount of unreacted diblock (15 % by deconvolution of the SEC chromatograms) contaminates the final P*N*VCL-*block*-P(*N*VCL-*stat*-*N*VP)-*b*-P*N*VCL triblock (Figure 1). The latter results from partial deactivation of the diblock chain-end before coupling.

In this way, we designed a series of *N*VCL and *N*VP di- and triblocks with various block lengths and compositions. Because copolymers with two discrete LCSTs are targeted, we ensured that the statistical P(*N*VCL-*stat*-*N*VP) segments of copolymers are *N*VP-rich (see Table 2) to make sure that their transition temperature sufficiently differs from the LCST of the P*N*VCL block.

Table 2. Characteristics of the *N*VCL and *N*VP containing di- and triblock copolymers prepared by CMRP and CMRC.

	P*N*VCL		P*N*VCL-*b*-P(*N*VCL-*stat*-*N*VP)				P*N*VCL-*b*-P(*N*VCL-*stat*-*N*VP)-*b*-P*N*VCL		
Entry	M_n [a] (g/mol)	Đ [a]	$M_{n\ P(NVCL\text{-}stat\text{-}NVP)}$ [a] (g/mol)	Đ [a]	*N*VCL (mol%) in the *stat* segment [b]	Label [c]	M_n [a] (g/mol)	Đ [a]	Label [c]
1	9500	1.07	31900	1.13	28	$C_{68}(C_{74}P_{191})$	64500	1.24	$C_{68}(C_{148}P_{382})C_{68}$
2	18400	1.05	24700	1.08	19	$C_{132}(C_{40}P_{172})$	71900	1.24	$C_{132}(C_{80}P_{344})C_{132}$
3	32800	1.06	24700	1.06	26	$C_{236}(C_{55}P_{154})$	110500	1.13	$C_{236}(C_{110}P_{308})C_{236}$
4	39200	1.06	37000	1.08	8	$C_{282}(C_{27}P_{297})$	128000	1.13	$C_{282}(C_{54}P_{594})C_{282}$

[a] Exact molar mass and dispersity determined by DMF-SEC using MALLS detector and RI detector with PS calibration, respectively. [b] Determined by ^{1}H NMR taking into account the exact molar mass of the P*N*VCL segment. [c] C and P designate *N*VCL and *N*VP, respectively. The numbers associated to these letters correspond to the degree of polymerization of each monomer. Detailed polymerization conditions are provided in Table S1.

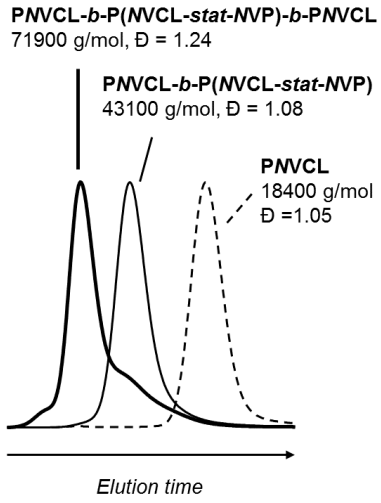

Figure 1. Overlay of the SEC chromatograms of the homoP*N*VCL precursor (C_{132}), the P*N*VCL-*block*-P(*N*VCL-*stat*-*N*VP) diblock ($C_{132}(C_{40}P_{172})$) and P*N*VCL-*block*-P(*N*VCL-*stat*-*N*VP)-*b*-P*N*VCL triblock ($C_{132}(C_{80}P_{344})C_{132}$) by sequential CMRP chain extension and CMRC (see Table 2, entry 2).

Thermoresponsive behaviour of the copolymers

In this section, the solution behaviour and the thermal response of the copolymers prepared above will be addressed starting with the statistical P(*N*VCL-*stat*-*N*VP) copolymers. As indicated by Table 1, the latter differ by their *N*VP/*N*VCL composition but their molar mass remains in the same range. The cloud point temperature (T_{CP}) of the aqueous solution of each copolymer (0.1 wt %) was measured by turbidimetry. The transmittance versus temperature plots, also called cloud point curves, are overlaid in Figure S2. A heating rate of 1 °C min^{-1} was used and we considered that the cloud point was reached when half of the transmittance of the solution was lost. The T_{CP} of each P(*N*VCL-*stat*-*N*VP) copolymer was then plotted as a function of their *N*VP molar fraction (Figure 2). For the sake of the comparison, the T_{CP} of a homoP*N*VCL (37 °C) was added on the graph. Because *N*VP is more hydrophilic than *N*VCL that contains two additional aliphatic carbons in the lactam ring, the higher is the *N*VP content in the copolymer, the higher is the phase transition temperature (Figure 2). For example, a T_{CP} of 72 °C was obtained when the *N*VP molar fraction in the copolymer was 0.57 (entry 5, Table 1). Note that no phase transition was detected below 100 °C for the copolymer containing 72 mol % of *N*VP (entry 6, Table 1). Although the dependence of the transition temperature with the *N*VP content does not appear to be linear, it is now possible to precisely tune the T_{CP} of a P(*N*VCL-*stat*-*N*VP) copolymer by adjusting its composition.

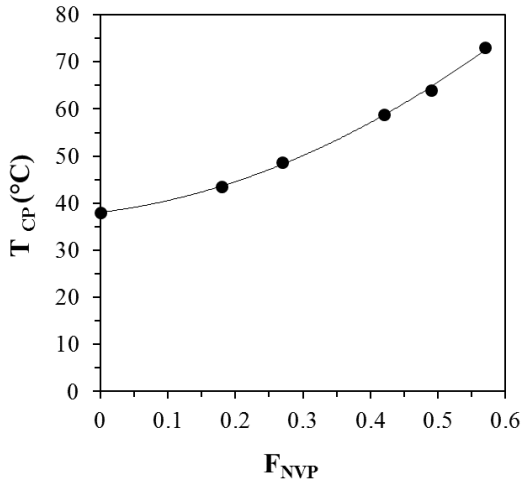

Figure 2. Evolution of the cloud point temperature (T_{CP}) of the statistical P(*N*VCL-*stat*-*N*VP) copolymer aqueous solutions (1 mg/mL) with the *N*VP molar fraction (F_{NVP}).

With these data in hand, we investigated the solution behaviour of the P*N*VCL-*block*-P(*N*VCL-*stat*-*N*VP) diblocks and P*N*VCL-*block*-P(*N*VCL-*stat*-*N*VP)-*block*-P*N*VCL triblocks. Theoretically, both types of copolymers should be double thermoresponsive, the T_{CP} of the P*N*VCL block(s) being inferior to the one of the *N*VP/*N*VCL statistical segment. Moreover, the transition temperature of one block could be influenced by the adjacent segment(s). Therefore, the impact of the copolymer architecture and composition on the T_{CP} of each segment is a key issue addressed in the present work as well as the organization of the di- and triblock copolymers in solution at different temperatures. Overall, an increase of the temperature is expected to change the solubility of the blocks in a stepwise fashion, inducing a multistep self-assembly behaviour described in scheme 4. Below (region **I**) and above (region **III**) both T_{CPS}, the copolymer chains should be fully soluble and aggregated in water, respectively. At intermediate temperatures (region **II**, $T_{CP1} < T < T_{CP2}$), only the P*N*VCL block precipitates leading to the self-organization of the copolymers in water. For most copolymers (see Table 2), the statistical P(*N*VCL-*stat*-*N*VP) segment is longer than the P*N*VCL block. Therefore, it is reasonable to expect the formation of spherical micelles composed of dehydrated P*N*VCL core stabilized by a P(*N*VCL-*stat*-*N*VP) corona, the latter consisting of loops in the case of the triblocks.

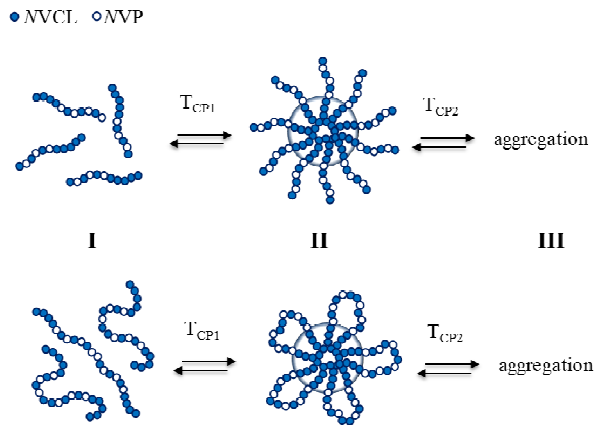

Scheme 4. Illustration of the thermally induced phase transitions of P*N*VCL-*block*-P(*N*VCL-*stat*-*N*VP) diblock and the corresponding P*N*VCL-*block*-P(*N*VCL-*stat*-*N*VP)-*block*-P*N*VCL triblock.

The thermal response of the block copolymers presented in Table 2 was systematically analysed by combination of turbidimetry and DLS. The study of the $C_{132}(C_{40}P_{172})$ and $C_{132}(C_{80}P_{344})C_{132}$ copolymer pair is presented in detail hereafter (Figures 3 and 4) while the transition temperatures of all the copolymers determined by a similar approach are collected and compared in Table 3.

Figure 3 shows the evolution of the transmittance (dotted line) and of the relative scattered light intensity (I/I_0) measured by DLS upon heating the aqueous solutions of $C_{132}(C_{40}P_{172})$ and $C_{132}(C_{80}P_{344})C_{132}$. For the diblock, two marked transitions are observed. The first one, indicated by the increase of the scattered intensity (full line in upper graph of Figure 3), appears around 45 °C. This transition corresponds to the selective precipitation of the P*N*VCL block (T_{CP1}). The latter occurs at higher temperature compared to a homoP*N*VCL (T_{CP} ~ 37 °C) because in the diblock the P*N*VCL is linked to a more hydrophilic sequence of P(*N*VCL-*stat*-*N*VP)[8]. The second phase transition was clearly identified by a sharp loss of transmittance at 70 °C, which is due to the dehydration and precipitation of the *N*VP containing segment. Importantly, the T_{CP} of the statistical P(*N*VCL-*stat*-*N*VP) sequence of the copolymer (70 °C) is drastically lowered by the more hydrophobic, and already collapsed, P*N*VCL block. Indeed, as mentioned above, an isolated *N*VCL/*N*VP statistical copolymer with the same composition (F_{NVP} = 0.81) should not exhibit a T_{CP} since we did not detect any for the P(*N*VCL-*stat*-*N*VP) with a *N*VP molar fraction of 0.72. The DLS size distribution histograms recorded at different temperatures are presented in Figure 4. At 35 °C (region **I**), the sample mainly consists of free chains, corresponding to the main peak being observed around a few nm. The second population, around 100 nm, is probably due to a small fraction of loose aggregates but is negligible being absent from the number-weighted size distribution graph (not shown). At 70 °C (region **III**), rather large objects are formed (~300 nm) suggesting complete aggregation of the copolymer chains. At 50 °C, so in region **II** corresponding to temperatures between the two T_{CPS}, micelles with an average hydrodynamic radius of 20 nm and a low polydispersity index (0.02) were observed. The morphology of the object has been tentatively studied by transmission electron microscopy (TEM) but aggregation occurred during the deposition on the TEM grid and evaporation of the thermostated solution (55 °C). Considering the copolymer composition, those are probably core-shell spherical micelles. Micelles with a very similar size were observed at several temperatures within region **II** (see Figure S3, for additional DLS curves). Interestingly enough, in the previously studied P*N*VCL-*block*-P(*N*VCL-*stat*-*N*MVA) copolymers, a transition region corresponding to the formation of large and ill-defined objects was observed prior micellization upon heating the copolymer solution.[34] In contrast, the present P*N*VCL-*block*-P(*N*VCL-*stat*-*N*VP) diblock exhibits a sharp unimers/micelles transition.

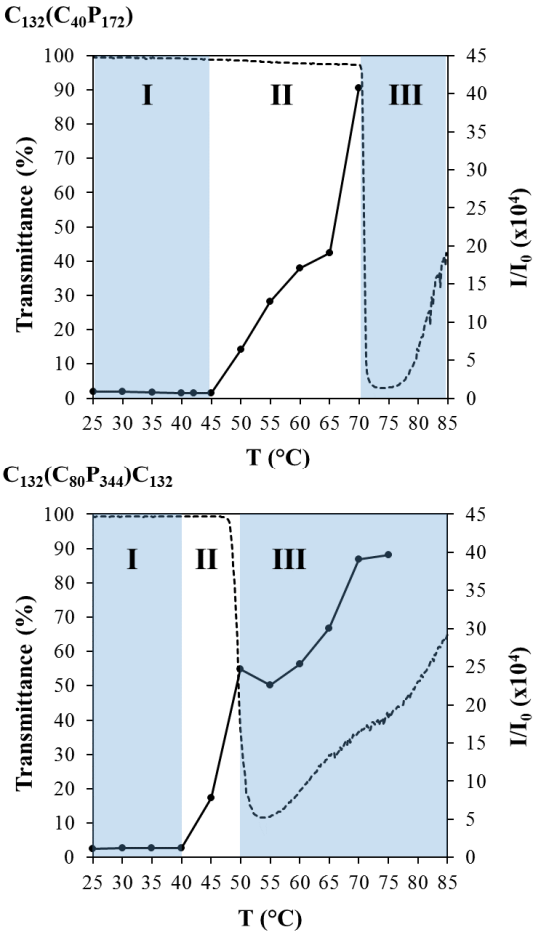

Figure 3. Transmittance (1 °C min^{-1}) (dotted line) and scattered intensity measured by DLS (full line) for the $C_{132}(C_{40}P_{172})$ diblock and the parent $C_{132}(C_{80}P_{344})C_{132}$ triblock aqueous solutions (1 g L^{-1}) as a function of temperature. See entry 2 in Table 2 for the detailed copolymer characteristics.

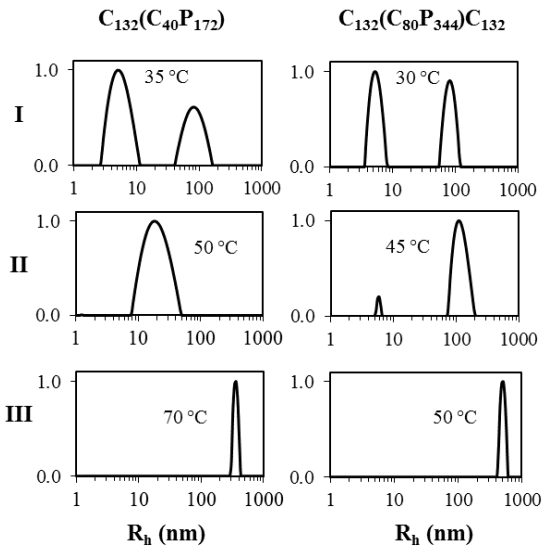

Figure 4. Intensity normalized CONTIN size distribution of P*N*VCL-*b*-P(*N*VCL-*stat*-*N*VP) diblock and the corresponding P*N*VCL-*b*-P(*N*VCL-*stat*-*N*VP)-*b*-P*N*VCL triblock aqueous solutions (1 g L^{-1}) at various temperatures (**I** below $T_{CP1\&2}$, **II** between T_{CP1} & T_{CP2}, **III** above $T_{CP1\&2}$). Additional DLS curves of the copolymers at other temperatures are provided in Figure S3.

Next, we examined the corresponding $C_{132}(C_{80}P_{344})C_{132}$ triblock under the same dilution condition (1 mg mL^{-1}). Again, two phase transitions were observed. The first one corresponds to the T_{CP} of the P*N*VCL external blocks of the copolymer and occurs around 40 °C as emphasized by the increase of the scattered light intensity measured by DLS (full line in lower graph of Figure 3). The second transition corresponds to the precipitation of the central P(*N*VCL-*stat*-*N*VP) segment of the triblock and was identified at 50 °C on the turbidimetry curve (dotted line in lower graph of Figure 3). The DLS size histograms presented in Figure 4 and S3 show that the triblock copolymer mainly exists as free chains below the first T_{CP} and is fully aggregated above the second T_{CP}, as for the diblock. In the inter-T_{CP} region, a major population around a hydrodynamic radius of about 100 nm is observed. This size seems too large to correspond to simple flower-like micelles, and the associated objects are probably small aggregates of micelles. The ABA triblock copolymer is indeed more prone to aggregation than the diblock because the A blocks can precipitate in two different micellar core, inducing the formation of bridges between micelles. Moreover, the self-assembly of the triblock in water is more difficult to control because the inter-T_{CP} window (region **II**) is much narrower compared to the diblock. Indeed, although the composition of the blocks of $C_{132}(C_{40}P_{172})$ and $C_{132}(C_{80}P_{344})C_{132}$ are strictly identical, their respective T_{CPS} vary from one architecture to another and are lower in the triblock than in the diblock (see Table 3). Doubling of the molar mass of the copolymer and of the statistical P(*N*VCL-*stat*-*N*VP) sequence by radical coupling might contribute to this effect. Nevertheless, considering previous reports[25] and the present range of molar mass variation, this factor should only be responsible for a decrease of few degree of the T_{CPS}. By contrast, the presence of a more hydrophobic P*N*VCL block at both extremities of the P(*N*VCL-*stat*-*N*VP) segment of the triblock should strongly decrease its transition temperature (from 70 °C in the diblock to 50 °C in the triblock). On the other hand, the hydrophobicity of the polymer chain linked to the P*N*VCL block, i.e. P(*N*VCL-*stat*-*N*VP) in the diblock and P(*N*VCL-*stat*-*N*VP)-*block*-P*N*VCL in the triblock, is globally higher in the triblock than the diblock. This might account for the lower T_{CP} of the P*N*VCL segment in the triblock (40 °C) compared to one in the diblock (45 °C) (see Table 3).

Following the same approach, we studied the thermal response of the aqueous solution of the other diblocks and triblocks mentioned in Table 2 which differ by their block length and compositions. All turbidimetry and DLS curves are provided in the supporting section (Figure S3-S10). The key transition temperatures of each copolymer are reported in Table 3 and discussed hereafter. Except for $C_{282}(C_{27}P_{297})$ and $C_{282}(C_{54}P_{594})C_{282}$, all copolymers exhibited a double thermoresponsive behaviour in water. Again, the T_{CPS} of both P*N*VCL block and of the *N*VP containing sequence were lower in the triblock than in the parent diblock. Moreover, the transition temperature of longer P*N*VCL block is less impacted by the hydrophilic P(*N*VCL-*stat*-*N*VP) segment. For example, considering the series of diblocks, the T_{CP} of the P*N*VCL was recorded at 50 °C, 45 °C and 40 °C for degrees of polymerization (DP) of P*N*VCL equal to 68, 132 and 236, respectively (Table 3). As a reminder the T_{CP} of homoP*N*VCL is around 37 °C. Interestingly, between T_{CP1} and T_{CP2}, $C_{68}(C_{74}P_{191})$, $C_{132}(C_{40}P_{172})$ and $C_{236}(C_{55}P_{154})$ formed well-defined micelles whose size increases with the length of the P*N*VCL segment. The R_h of the micelles are equal to 15 nm, 20 nm and 30 nm for DP of 68, 132 and 236, respectively (Figures S5, S3 and S7). On the other hand, the study of the $C_{68}(C_{148}P_{382})C_{68}$ and $C_{236}(C_{110}P_{308})C_{236}$ triblocks confirmed the difficulty to form well defined objects and to avoid aggregation.

Table 3. T_{CPS} of the *N*VCL/*N*VP-based di- and triblocks.

Copolymers	T_{CP1} (°C) [a]	T_{CP2} (°C) [b]
$C_{68}(C_{74}P_{191})$	50	70
$C_{68}(C_{148}P_{382})C_{68}$	52	58
$C_{132}(C_{40}P_{172})$	45	70
$C_{132}(C_{80}P_{344})C_{132}$	40	50
$C_{236}(C_{55}P_{154})$	40	67
$C_{236}(C_{110}P_{308})C_{236}$	40	43
$C_{282}(C_{27}P_{297})$	35	/ [c]
$C_{282}(C_{54}P_{594})C_{282}$	40	/ [c]
$C_{282}(C_{27}P_{297})$	25 [d]	63 [d]
$C_{282}(C_{54}P_{594})C_{282}$	25 [d]	68 [d]

Copolymer aqueous solutions (1 g/L) [a] T_{CP1} values correspond to the onset temperature of the increase of the scattered light intensity measured by DLS (as shown in Figure 3).[b] T_{CP2} is measured at 50% of transmittance loss on the turbidimetry curves. [c] No second T_{CP} was detected below 95 °C. [d] Determined in 2 M NaCl aqueous solution.

For $C_{282}(C_{27}P_{297})$ and $C_{282}(C_{54}P_{594})C_{282}$, no precipitation was observed in water below 95 °C because the *N*VP content in their statistical block was too high (F_{NVP} = 0.92), suppressing the second T_{CP}. However, the T_{CP} of the P*N*VCL segment in the diblock (Figure 5) and in the triblock (Figure S8) was detected around 40 °C. These copolymers mainly exist as free chains below 40 °C and self-assembled above the transition temperature. Narrowly dispersed micelles with a R_h of about 30 nm were observed for $C_{282}(C_{27}P_{297})$ between 40 °C and 90 °C (Figure S9). In the same range of temperatures, $C_{282}(C_{27}P_{594})C_{282}$ led to assemblies with a hydrodynamic radius between 25 and 35 nm, which probably correspond to flower-like micelles, as well as larger aggregates (R_h~200 nm) (Figure S9).

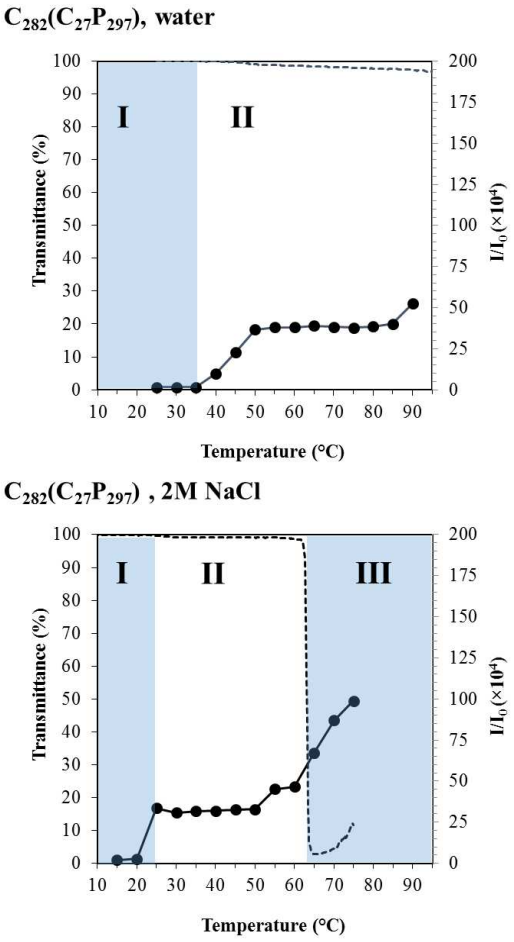

Figure 5. Transmittance (1 °C min^{-1}) (dotted line) and scattered intensity measured by DLS (full line) for the $C_{282}(C_{27}P_{297})$ diblock (1 g L^{-1}) in water and in 2M NaCl aqueous solutions as a function of temperature.

The polymer solubility, and LCST of thermoresponsive macromolecules in particular, can be strongly influenced by the presence of salts in the aqueous solution.[68, 69] In particular, hydration and phase behaviour of P*N*VCL and P*N*VP in water are known to be impacted by the presence of salts which decreases their LCSTs.[65] This salting out effect was here used to change the T_{CP} of the P*N*VCL segment of $C_{282}(C_{27}P_{297})$ and of $C_{282}(C_{54}P_{594})C_{282}$ and to possibly decrease the solubility of the statistical P(*N*VCL-*stat*-*N*VP) segment, revealing a second T_{CP} below 100 °C and providing thus double thermoresponsiveness to the copolymer. In a 2 M NaCl aqueous solution, $C_{282}(C_{27}P_{297})$ indeed showed two T_{CPS} (25 °C and 63 °C, Figure 5) and micelles with a hydrodynamic radius of about 35 nm were observed in the inter-T_{CP} window (Figure S10). Addition of salt also shifted downwards the T_{CPS} of $C_{282}(C_{54}P_{594})C_{282}$ and for the first time the temperature range of the inter-T_{CP} window was rather large (between 25 °C and 67 °C) (Figure S8 and S10). In conclusion, the salting out effect thus appears to be a very useful tool to adjust the transition temperature of *N*VCL and *N*VP-based double thermoresponsive block copolymers.

Finally, the reversibility of the temperature induced phase transitions was investigated by turbidimetry for $C_{282}(C_{27}P_{297})$ and $C_{282}(C_{54}P_{594})C_{282}$ in a 2M NaCl aqueous solution. For the diblock, the T_{CPS} observed upon heating and cooling the solutions were quite similar and hysteresis did not exceed a few degrees (Figure S11). Moreover, the objects formed in solution when increasing and decreasing the temperature were similar (Figure S12) although the micelles detected in the inter-T_{CP} region were larger when cooling the solution. Indeed, the R_h of the micelles observed at 45 °C were around 35 nm and 60 nm in the heating and cooling phases, respectively (Figure S12). In such experiments, kinetically frozen micelles are most probably formed considering the abrupt character of the LCST transition. It is therefore not surprising to observe micelles of different sizes during heating and cooling, since it is well-known that the preparation protocol may strongly influence the micellar characteristics in the case of kinetically frozen micelles.[70] In the case of the triblock $C_{282}(C_{54}P_{594})C_{282}$, as indicated by the turbidimetry curves (Figure S11), the re-solubilisation of the copolymer when cooling the solution was difficult, which prevent us from performing a size analysis by DLS. Nonetheless, its double thermo-responsive character is demonstrated in both the heating and cooling cycles.

Conclusion

A series of novel well-defined thermoresponsive *N*VCL and *N*VP-based copolymers, including statistical, diblock and triblock copolymers, were prepared by cobalt-mediated radical polymerization (CMRP) and coupling reaction (CMRC). Due to the high level of control on the molecular parameters of the polymers it was possible to compare their thermal properties based on their composition, block length, and architecture. Increasing the *N*VP content in statistical *N*VCL/*N*VP copolymers was shown to increase their lower critical solution temperature in water, 0.7 being approximately the maximum *N*VP molar fraction for maintaining the T_{CP} of such statistical copolymers below 90 °C. With these data in hands, four pairs of double thermoresponsive di- and triblock composed of P*N*VCL and P(*N*VCL-*stat*-*N*VP) blocks were obtained by sequential CMRP of *N*VCL and *N*VCL/*N*VP polymerizations followed by radical coupling with isoprene. In both types of architecture, the thermal response of P*N*VCL and of the P(*N*VCL-*stat*-*N*VP) segment influenced each other, the LCST of the P*N*VCL block being increased by the more hydrophilic

P(*N*VCL-*stat*-*N*VP) block and vice versa. As a general trend, the inter-T_{CP} region was narrower and occurred at lower temperature for the triblock because the central *N*VCL/*N*VP block is linked to P*N*VCL at both extremities. In the case of the diblocks, narrowly dispersed micelles were formed from unimers upon heating, and total collapse occurred above the second T_{CP}, confirming the multistep assembly behaviour of the copolymers. For the triblocks, the self-assembly was more difficult to control due to their enhanced tendency to aggregation, linked to their ABA structure, and the narrower inter-T_{CP} window. Moreover, the NaCl salting-out effect was successfully used to adjust the T_{CPS} of these types of copolymers to the extent that the T_{CP} of a *N*VP rich statistical segment became detectable below 100 °C, making the corresponding di- and triblock double thermoresponsive. Finally, the double thermo-responsive character of the *N*VCL and *N*VP-based copolymers was also emphasized in both the heating and cooling cycles. As a result, the data presented here provide a basis to synthesize a broad range of double thermoresponsive *N*VCL- and *N*VP-based di- and triblock copolymers with tunable LCSTs and highlight the crucial impact of the architecture of the copolymer on their thermal phase transition.

Acknowledgments

The authors are grateful to the "Fonds National de la Recherche Scientifique" (FRS-FNRS) and to the Belgian Science Policy for financial support in the frame of the Interuniversity Attraction Poles Program (P7/05)–Functional Supramolecular Systems (FS2) for financial support. A.D. is also grateful for fundings from the University of Liège via the "Fonds spéciaux pour la recherche". A.D. and C.A.F. are Research Associates of the FRS- FNRS, and C.D. is Research Director of the FRS-FNRS. R.D. thanks FRIA for PhD fellowship. The authors also thank G. Cartigny and A. Matagne, for skilful assistance in MALLS and for giving access to the turbidimetry analysis, respectively.

Notes and references

[a] *Center for Education and Research on Macromolecules (CERM), Chemistry Department, University of Liege (ULg), Sart-Tilman, Allée de la Chimie 3, Bat. B6a, B-4000 Liège, Belgium. Tel : (32)43663565, e-mail : adebuigne@ulg.ac.be*

[b] *Institute of Condensed Matter and Nanosciences (IMCN), Bio- and Soft Matter division (BSMA), Université Catholique de Louvain, Place Pasteur 1, 1348 Louvain-la-Neuve, Belgium.*

† Electronic Supplementary Information (ESI) available: Additional structural characterizations and the thermal response studies of the copolymers were carried out by nuclear magnetic resonance, turbidimetry, dynamic light scattering.

1. F. Liu and M. W. Urban, *Prog. Polym. Sci.*, 2010, 35, 3-23.
2. A. E. Smith, X. Xu and C. L. McCormick, *Prog. Polym. Sci.*, 2010, 35, 45-93.
3. D. Roy, J. N. Cambre and B. S. Sumerlin, *Prog. Polym. Sci.*, 2010, 35, 278-301.
4. C. d. l. H. Alarcon, S. Pennadam and C. Alexander, *Chem. Soc. Rev.*, 2005, 34, 276-285.
5. A. S. Hoffman, *Adv. Drug Delivery Rev.*, 2013, 65, 10-16.
6. E. S. Gil and S. M. Hudson, *Prog. Polym. Sci.*, 2004, 29, 1173-1222.
7. D. Roy, W. L. A. Brooks and B. S. Sumerlin, *Chem. Soc. Rev.*, 2013, 42, 7214-7243.
8. V. Aseyev, H. Tenhu and F. M. Winnik, *Adv. Polym. Sci.*, 2011, 242, 29-89.
9. I. Dimitrov, B. Trzebicka, A. H. E. Mueller, A. Dworak and C. B. Tsvetanov, *Prog. Polym. Sci.*, 2007, 32, 1275-1343.
10. S.-I. Yusa, S. Awa, M. Ito, T. Kawase, T. Takada, K. Nakashima, D. Liu, S. Yamago and Y. Morishima, *J. Polym. Sci. Polym. Chem.* , 2011, 49, 2761-2770.
11. S. Reinicke, P. Espeel, M. M. Stamenović and F. E. Du Prez, *ACS Macro Letters*, 2013, 2, 539-543.
12. E. A. Clark and J. E. G. Lipson, *Polymer*, 2012, 53, 536-545.
13. J.-F. Lutz, *Adv. Mater.*, 2011, 23, 2237-2243.
14. G. Vancoillie, D. Frank and R. Hoogenboom, *Prog. Polym. Sci.*, 2014, 39, 1074–1095.
15. Y.-C. Wang, H. Xia, X.-Z. Yang and J. Wang, *J. Polym. Sci., Part A: Polym. Chem.*, 2009, 47, 6168-6179.
16. E. A. Yapar and O. Ynal, *Trop. J. Pharm. Res.*, 2012, 11, 855-866.
17. O. Confortini and F. E. Du Prez, *Macromol. Chem. Phys.*, 2007, 208, 1871-1882.
18. Y. Maeda, *Langmuir*, 2001, 17, 1737-1742.
19. R. Hoogenboom, *Angew. Chem., Int. Ed.*, 2009, 48, 7978-7994.
20. L. T. T. Trinh, H. M. L. Lambermont-Thijs, U. S. Schubert, R. Hoogenboom and A.-L. Kjoeniksen, *Macromolecules* 2012, 45, 4337-4345.
21. H. Cheng, L. Shen and C. Wu, *Macromolecules*, 2006, 39, 2325-2329.
22. H. G. Schild, *Prog. Polym. Sci.*, 1992, 17, 163-249.
23. H. Vihola, A. Laukkanen, L. Valtola, H. Tenhu and J. Hirvonen, *Biomaterials*, 2005, 26, 3055-3064.
24. H. Vihola, A. Laukkanen, H. Tenhu and J. Hirvonen, *J. Pharm. Sci.*, 2008, 97, 4783-4793.
25. F. Meeussen, E. Nies, H. Berghmans, S. Verbrugghe, E. Goethals and F. Du Prez, *Polymer*, 2000, 41, 8597-8602.
26. S.-T. Sun and P.-Y. Wu, *J. Phys. Chem. B*, 2011, 115, 11609-11618.
27. L. M. Mikheeva, N. V. Grinberg, A. Y. Mashkevich, V. Y. Grinberg, L. T. M. Thanh, E. E. Makhaeva and A. R. Khokhlov, *Macromolecules*, 1997, 30, 2693-2699.
28. Y. Gao, S. C. F. Au-Yeung and C. Wu, *Macromolecules*, 1999, 32, 3674-3677.
29. S. F. Medeiros, J. C. S. Barboza, R. Giudici and A. M. Santos, *J. Macromol. Sci., Part A: Pure Appl. Chem.*, 2013, 50, 763-773.
30. L. Shao, M. Hu, L. Chen, L. Xu and Y. Bi, *React. Funct. Polym.*, 2012, 72, 407-413.
31. M. Beija, J.-D. Marty and M. Destarac, *Chem. Commun.* , 2011, 47, 2826-2828.
32. D. Wan, Q. Zhou, H. Pu and G. Yang, *J. Polym. Sci., Part A: Polym. Chem.*, 2008, 46, 3756-3765.
33. S. M. Ponce-Vargas, N. A. Cortez-Lemus and A. Licea-Claverie, *Macromol. Symp.*, 2013, 325-326, 56-70.
34. A. Kermagoret, C.-A. Fustin, M. Bourguignon, C. Detrembleur, C. Jérôme and A. Debuigne, *Polym. Chem.*, 2013, 4, 2575-2583.
35. J. Liu, C. Detrembleur, M.-C. De Pauw-Gillet, S. Mornet, E. Duguet and C. Jerome, *Polym. Chem.*, 2014, 5, 799-813.
36. Y. C. Yu, G. Li, J. Kim and J. H. Youk, *Polymer*, 2013, 54, 6119-6124.
37. Y. C. Yu, H. U. Kang and J. H. Youk, *Colloid Polym. Sci.*, 2012, 290, 1107-1113.
38. W. Tian, X. Lv, L. Huang, N. Ali and J. Kong, *Macromol. Chem. Phys.*, 2012, 213, 2450-2463.
39. M. Hurtgen, J. Liu, A. Debuigne, C. Jérôme and C. Detrembleur, *J. Polym. Sci., Part A: Polym. Chem.*, 2012, 50, 400-408.
40. J. Liu, C. Detrembleur, A. Debuigne, M.-C. De Pauw-Gillet, S. Mornet, L. Vander Elst, S. Laurent, E. Duguet and C. Jérôme, *J. Mater. Chem. B*, 2014, 2, 1009-1023.
41. J. Liu, C. Detrembleur, M. Hurtgen, A. Debuigne, M.-C. De Pauw-Gillet, S. Mornet, E. Duguet and C. Jérôme, *Polym. Chem.*, 2014,

5, 77-88.
42. X. Jiang, Y. Li, G. Lu and X. Huang, *Polym. Chem.*, 2013, 4, 1402-1411.
43. X. Jiang, G. Lu, C. Feng, Y. Li and X. Huang, *Polym. Chem.*, 2013, 4, 3876-3884.
44. K. Nakabayashi and H. Mori, *Eur. Polym. J.*, 2013, 49, 2808-2838.
45. I. Negru, M. Teodorescu, P. O. Stanescu, C. Draghici, A. Lungu and A. Sarbu, *Mater. Plast.* , 2010, 47, 35-41.
46. P. Singh, A. Srivastava and R. Kumar, *J. Polym. Sci., Part A: Polym. Chem.*, 2012, 50, 1503-1514.
47. M. Hurtgen, C. Detrembleur, C. Jérôme and A. Debuigne, *Polym. Rev.* , 2011, 51, 188-213.
48. A. Debuigne, R. Poli, C. Jérôme, R. Jérôme and C. Detrembleur, *Prog. Polym. Sci.*, 2009, 34, 211-239.
49. A. Debuigne, A. N. Morin, A. Kermagoret, Y. Piette, C. Detrembleur, C. Jérôme and R. Poli, *Chem. - Eur. J.*, 2012, 18, 12834-12844.
50. Y.-G. Jia and X. X. Zhu, *Polym. Chem.*, 2014, 5, 4358-4364.
51. A. M. Bivigou-Koumba, J. Kristen, A. Laschewsky, P. Mueller-Buschbaum and C. M. Papadakis, *Macromol. Chem. Phys.*, 2009, 210, 565-578.
52. Z. Ge, Y. Zhou, Z. Tong and S. Liu, *Langmuir*, 2011, 27, 1143-1151.
53. K. Skrabania, W. Li and A. Laschewsky, *Macromol. Chem. Phys.*, 2008, 209, 1389-1403.
54. X. Zhao, W. Liu, D. Chen, X. Lin and W. W. Lu, *Macromol. Chem. Phys.*, 2007, 208, 1773-1781.
55. S. E. Kirkland, R. M. Hensarling, S. D. McConaughy, Y. Guo, W. L. Jarrett and C. L. McCormick, *Biomacromolecules*, 2008, 9, 481-486.
56. E. Hasan, M. Zhang, A. Mueller and C. B. Tsvetanov, *J. Macromol. Sci., Pure Appl. Chem.*, 2004, A41, 467-486.
57. X. Chen, X. Ding, Z. Zheng and Y. Peng, *Colloid Polym. Sci.*, 2005, 283, 452-455.
58. F. Dai, P. Wang, Y. Wang, L. Tang, J. Yang, W. Liu, H. Li and G. Wang, *Polymer*, 2008, 49, 5322-5328.
59. K. Skrabania, J. Kristen, A. Laschewsky, O. Akdemir, A. Hoth and J.-F. Lutz, *Langmuir*, 2007, 23, 84-93.
60. A. Debuigne, C. Jérôme and C. Detrembleur, *Angew. Chem., Int. Ed.*, 2009, 48, 1422-1424.
61. A. Debuigne, R. Poli, J. De Winter, P. Laurent, P. Gerbaux, P. Dubois, J.-P. Wathelet, C. Jérôme and C. Detrembleur, *Chem. - Eur. J.*, 2010, 16, 1799-1811.
62. A. Debuigne, R. Poli, J. De Winter, P. Laurent, P. Gerbaux, J.-P. Wathelet, C. Jérôme and C. Detrembleur, *Macromolecules* 2010, 43, 2801-2813.
63. A. Debuigne, Y. Champouret, R. Jérôme, R. Poli and C. Detrembleur, *Chem.- Eur. J.*, 2008, 14, 4046-4059.
64. A. Debuigne, J.-R. Caille and R. Jérôme, *Macromolecules*, 2005, 38, 5452-5458.
65. Y. Maeda, T. Nakamura and I. Ikeda, *Macromolecules*, 2002, 35, 217-222.
66. E. E. Sokorikova, T. M. Karaputadze, A. M. Ovsepyan, A. I. Aksenov and Y. E. Kirsh, *Vysokomol. Soedin., Ser. B*, 1985, 27, 869-871.
67. A. Kermagoret, A. Debuigne, C. Jérôme and C. Detrembleur, *Nat. Chem.* , 2014, 6, 179-187.
68. R. Sadeghi and F. Jahani, *J. Phys. Chem. B*, 2012, 116, 5234-5241.
69. M. M. Bloksma, D. J. Bakker, C. Weber, R. Hoogenboom and U. S. Schubert, *Macromol. Rapid Commun.*, 2010, 31, 724-728.
70. R. C. R. C. Hayward and D. J. Pochan, *Macromolecules* 2010, 43, 3577-3584.